

Two-photon absorption in ZnSe and ZnSe/ZnS core/shell quantum structures

Amit D. Lad,¹ P. Prem Kiran,^{2,a)} Deepak More,^{1,b)} G. Ravindra Kumar,^{2,c)} and Shailaja Mahamuni^{1,d)}

¹Department of Physics, University of Pune, Pune 411007, India

²Tata Institute of Fundamental Research, Mumbai 400005, India

(Received 3 September 2007; accepted 2 January 2008; published online 31 January 2008)

The third order nonlinear optical properties of two different sized ZnSe and ZnSe/ZnS quantum dots (QDs) are investigated. The nonlinear absorption is measured at 806 nm using Ti:sapphire 100 fs laser pulses in an open aperture Z-scan setup. Two-photon absorption (2PA) is found to be dominant in core and core shell QDs. 2PA cross section is enhanced by three orders of magnitude compared bulk ZnSe. 2PA cross section is observed to increase with reduction in QD diameter, due to strong confinement effect. ZnSe/ZnS QDs exhibit higher 2PA cross section compared with corresponding ZnSe QDs, indicating better passivation of the QD surface. © 2008 American Institute of Physics. [DOI: 10.1063/1.2839400]

Recently, third order optical nonlinearity in various semiconductor quantum dots^{1–10} (QDs) has been studied in great detail due to potential application in biological imaging, ultrafast optical switching, optical limiting, and optoelectronic devices. ZnSe QDs are promising candidate for various optoelectronic devices¹¹ and, hence in this letter, nonresonant third order nonlinear optical properties of ZnSe and ZnSe/ZnS QDs are investigated.

Two-photon absorption (2PA) is found to be enhanced in various semiconductor QDs (Refs. 3–8) in comparison with their respective bulk counterparts. However, ZnSe QDs embedded in glass matrix¹ exhibit the absence of nonlinear absorption (NLA). Our earlier communication¹² reveals three-photon absorption (3PA) cross section in ZnSe and ZnSe/ZnS QDs to be four orders of magnitude larger than that in bulk ZnSe. Also, an increase in 3PA cross section is observed in case of core/shell QDs compared with its core. In case of CdSe/ZnS QDs, Wang *et al.*⁶ observed twice an increase in value of $\chi^{(3)}$ as compared with bare CdSe QDs. These evidences indicate that the surface of the nanocrystal plays an important role in determination of its nonlinear optical properties.

ZnSe QDs of two different sizes were synthesized¹³ by injecting diethylzinc and trioctylphosphine (TOP) selenide at different temperatures in hexadecylamine (HDA). A monolayer of ZnS shell on ZnSe QDs was capped to nullify the surface effects by the method described by Dabbousi *et al.*¹⁴ NLA was measured in an open aperture Z-scan setup, using a Ti-sapphire laser emitting 806 nm (1.54 eV), 100 fs pulses at 10 Hz repetition rate. NLA studies under these conditions reveal the potential for ultrafast optoelectronic applications by avoiding the thermal contributions. The open aperture Z-scan setup was similar to that used in Ref. 12. The laser beam was focused using a lens of 35 cm, giving the focal spot size of 57 μm . The peak intensities incident on the

sample were maintained between 8 and 30 GW/cm^2 to avoid the damage. QDs were dispersed in *n*-butanol and placed in 1 mm quartz cuvette. Z scan of capping agents (TOP and HDA) in *n*-butanol was performed to verify that the NLA is only due to QDs and not from organic capping agents.

The x-ray diffraction (XRD) study reveals zinc blende cubic structure for ZnSe as well as for ZnSe/ZnS QDs.¹² Size of ZnSe I and ZnSe/ZnS I as determined from XRD is 4.5 ± 0.6 nm, whereas size of ZnSe II and ZnSe/ZnS II is 3.5 ± 0.4 nm. Transmission electron microscopic images indicate the formation of ZnS shell of thickness with about 0.2 nm around ZnSe QDs.¹² The linear optical absorptions [Fig. 1(a)] of ZnSe I and ZnSe/ZnS I QDs exhibit the lowest excitonic transition $1S_{3/2}^h - 1S^e$ (forbidden gap) at 410 nm (3.02 eV). The same excitonic transition for ZnSe II and ZnSe/ZnS II QDs is located at 382 nm (3.25 eV). Quantum size effects are clearly revealed from the linear absorption spectra. The sizes derived from tight-binding calculations¹⁵

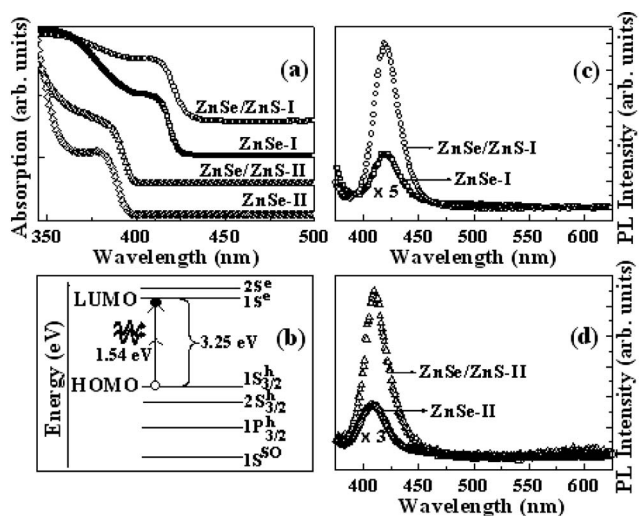


FIG. 1. (a) Linear optical absorption spectra of ZnSe and ZnSe/ZnS core/shell QDs. (b) Schematic of electron energy levels and 2PA mechanism in ZnSe QDs. Room temperature PL spectra measured with excitation wavelength of 350 nm for (c) ZnSe I and ZnSe/ZnS I QDs, (d) ZnSe II, and ZnSe/ZnS II QDs.

^{a)}Present address: Advanced Centre of Research in High Energy Materials, University of Hyderabad, Hyderabad 500046, India.

^{b)}Permanent address: K. J. Somaiya College of Science and Commerce, Mumbai 400077, India.

^{c)}Electronic mail: grk@tifr.res.in.

^{d)}Electronic mail: shailajamahamuni@yahoo.co.in.

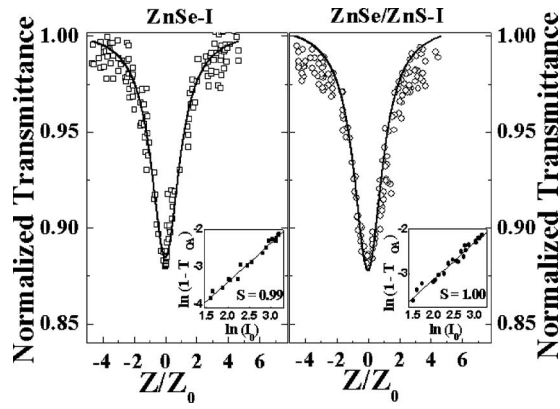


FIG. 2. Open aperture Z-scan curves of ZnSe I and ZnSe/ZnS I QDs at input intensity of 24.2 GW/cm². The insets show the scaling for 2PA.

for ZnSe I and ZnSe/ZnS I QDs is 4.3 nm and for ZnSe-II and ZnSe/ZnS II QDs is 3.3 nm. Various excitonic states of ZnSe QDs have been mapped by using photoluminescence excitation spectroscopy.¹⁶ Figure 1(b) exhibits the availability of $1S_{3/2}^h - 1S^e$ state to absorb two photons with energy 1.54 eV simultaneously. Figure 1(c) shows the PL measurement of ZnSe I and ZnSe/ZnS I QDs. The band-edge emission is centered at 420 nm. The relative quantum efficiency (QE) of QDs is measured with respect to the PL of stilbene laser dye. The QE of ZnSe I QDs is 2%, whereas an 11 times increase in QE is observed for ZnSe I QDs overcoated with a ZnS shell. The QE of ZnSe II QDs is 2%, whereas ZnSe/ZnS II QDs exhibit QE to 17%. The band-edge emission in case of ZnSe II and ZnSe/ZnS II is centered at 408 nm [Fig. 1(d)]. The increase in QE is attributed to better-passivated QD surface and localization of the holes in the core region.¹⁷ The increase in QE further confirms the formation of ZnS shell and electronic passivation of ZnSe QD surface.

The open aperture Z-scan traces at input intensity of 24.2 GW/cm² are shown in Figs. 2 and 3. The valley feature with minimum transmittance at the focus ($Z=0$), clearly indicates the presence of NLA in our QDs. The insets in Figs. 2 and 3 represent the logarithmic plot of $(1-T_{OA})$ (where T_{OA} is open aperture transmittance) versus I_0 (excitation intensity of laser beam at focus). These show the slope nearly unity for all the QDs, confirming that two photons have been simultaneously absorbed by these QDs. Enhanced 2PA due to the quantum size effects from ZnSe I to ZnSe II is evident from the Figs. 2(a) and 3(a). For ZnSe I QDs, the normalized absorbance at focus ($A_{z=0}=1-T_{z=0}$) is around 0.11 and for

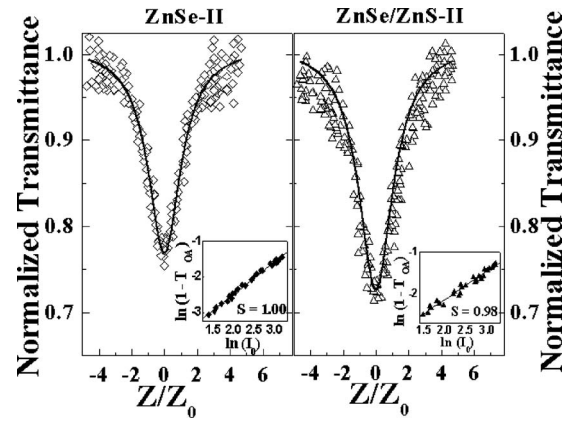


FIG. 3. Open aperture Z-scan curves of ZnSe II and ZnSe/ZnS II QDs at input intensity of 24.2 GW/cm². The insets show the scaling for 2PA.

ZnSe II $A_{z=0}$ is around 0.23. A similar increase of $A_{z=0}$ of 0.13 from ZnSe/ZnS I to $A_{z=0}$ of 0.27 ZnSe/ZnS II is observed for the core/shell QDs. By assuming a spatially and temporally Gaussian profile for laser beam, the normalized energy transmittance $T_{OA}(Z)$, for 2PA can be given as¹⁸

$$T_{OA}(Z) = \frac{1}{\sqrt{\pi}q_0} \int_{-\infty}^{\infty} \ln[1 + q_0 \exp(-x^2)] dx, \quad (1)$$

where $q_0 = \beta_2 I_0 L_{eff}$, β_2 is 2PA coefficient, $L_{eff} = [1 - \exp(-\alpha l)] / \alpha$, α is linear absorption coefficient, and l is the sample path length. The 2PA coefficient can be obtained by fitting the open aperture Z-scan traces by using Eq. (1). Figures 2 and 3 indicate that theoretical curve (solid line) matches well with the experimental data (symbols). 2PA per QD (β_{2QD}) has been evaluated and summarized in Table I. 2PA is related to third order susceptibility [$\chi^{(3)}$] by $\beta_2 = 4\pi \text{Im} \chi^{(3)} / (\lambda n_0^2 c \epsilon_0)$, where n_0 is linear refractive index, λ is wavelength of laser, c is speed of light in vacuum, and ϵ_0 is dielectric constant of the material.² The intrinsic 2PA coefficient of QDs (γ_{QD}) can be deduced as $\gamma_{QD} = \beta_{2solution} n_{0solution}^2 / (n_{0QD}^2 f_v |f|^4)$, where f_v is volume fraction of QDs in the solution, and f is local field correction depending upon the dielectric constant of material and solution. The enhancement in intrinsic 2PA coefficient (Table I) is observed with reduction in size of the QD due to quantum confinement effects.¹⁹

From the 2PA coefficient (β_2), 2PA cross section (σ_2) can be deduced⁷ using the relation $\sigma_2 = \beta_2 h\nu / N_0$ where N_0 is number density of QDs dispersed in the solution. We have

TABLE I. Linear optical absorption, QD diameter, 2PA coefficient per QD, intrinsic 2PA coefficient, and 2PA cross section of the core and core/shell QDs dispersed in *n*-butanol.

	Linear absorption (eV)	Diameter estimated by XRD (nm)	2PA coefficient per QD β_{2QD} (cm/GW)	Intrinsic 2PA coefficient γ_{QD} (cm/GW)	2PA cross section σ_2 (GM)
ZnSe I	3.02	4.5	7.9×10^{-14}	2.10	0.49×10^4
ZnSe/ZnS I	3.02	4.5	8.2×10^{-14}	2.17	0.51×10^4
ZnSe II	3.25	3.5	19.5×10^{-14}	5.16	1.22×10^4
ZnSe/ZnS II	3.25	3.5	22.2×10^{-14}	5.88	1.39×10^4
ZnS QDs ^a	4.77	1.8	0.937×10^{-14}		1.72×10^4
Bulk ZnSe ^b	2.67				69.4

^aReference 3.

^bReference 20.

maintained constant $N_0=4.2\times 10^{17}\text{ cm}^{-3}$. 2PA cross section of ZnSe I and ZnSe II is found to be 0.49×10^4 and 1.22×10^4 GM, where $\text{GM}=10^{-50}\text{ cm}^4\text{ s/photon}$. Also, 2PA cross sections of ZnSe/ZnS I and ZnSe/ZnS II is found to be 0.51×10^4 and 1.39×10^4 GM (Table I). The typical enhancement of 2PA cross section is also observed in ZnS,³ CdS,⁴ CdSe,⁷ and CdTe (Ref. 8) QDs. 2PA cross section is found to be three magnitudes higher in ZnSe QDs as compared with bulk ZnSe.²⁰ It may also be noted that 2PA cross section in ZnSe QDs is comparable to that of the ZnS,³ CdS,⁴ and CdTe (Ref. 8) QDs. The enhancement in 2PA cross section has been observed in case of ZnSe/ZnS core/shell quantum structure compared to that of core ZnSe QDs. The enhancement in nonlinear properties can be attributed to an electronic passivation of QD surface and the localization of charge carriers in core/shell quantum heterostructure.¹² Furthermore, an increase in nonlinearity is observed with decrease in QD diameter. This is consistent with the established result that an increase in exciton oscillator strength with decrease in QD size is responsible for an improvement in nonlinearity.¹⁹ Mn-doped ZnSe nanocrystals¹⁰ exhibit increase in 2PA coefficient with increase in overcoating ZnSe shell thickness. However, recent studies on CdTe QDs embedded in borosilicate glass,⁹ CdSe QDs dispersed in methanol and octadecene,⁹ and water soluble thiol capped CdTe QDs (Ref. 8) show decrease in 2PA cross section with decrease in QD diameter. These point out that the dependence of 2PA cross section on the size of the QD needs to be understood further. We are carrying out more studies in this direction.

In summary, 2PA is found to be a dominant mechanism in ZnSe and ZnSe/ZnS QDs at incident excitation photon energy of 1.54 eV. 2PA cross section is found to be enhanced by three orders of magnitude as compared with bulk ZnSe. QD surface is found to be active in determination of optical nonlinearity as 2PA coefficient in core/shell QDs is larger than its respective core QDs. The increase in nonlinearity with decrease in QD diameter is attributed to quantum size effects. We observe considerable 2PA (with 100 fs, 806 nm

laser pulses) and when we couple these observations together with our earlier measurements¹² of significant 3PA (with 35 ps, 1064 nm laser pulses), these QD systems appear to have great potential in ultrafast switching and optical limiting devices in a broad spectral region near infra red.

Financial support by DST is gratefully acknowledged. G.R.K. acknowledges a DAE-SRC-ORI grant. The authors are thankful to Ch. Rajesh for the help in the experiments.

¹Y.-C. Ker, J.-H. Lin, and W.-F. Hsieh, *Jpn. J. Appl. Phys., Part 1* **42**, 1258 (2003).

²J. He, W. Ji, G. H. Ma, S. H. Tang, H. I. Elim, W. X. Sun, Z. H. Zhang, and W. S. Chin, *J. Appl. Phys.* **95**, 6381 (2004).

³V. V. Nikesh, A. Dharmadhikari, H. Ono, S. Nozaki, G. R. Kumar, and S. Mahamuni, *Appl. Phys. Lett.* **84**, 4602 (2004).

⁴J. He, J. Mi, H. Li, and W. Ji, *J. Phys. Chem. B* **109**, 19184 (2005).

⁵I. Gerdova and A. Haache, *Opt. Commun.* **26**, 205 (2005).

⁶X. Wang, Y. Du, S. Ding, Q. Wang, G. Xiang, M. Xie, X. Chen, and D. Peng, *J. Phys. Chem. B* **110**, 1566 (2006).

⁷Y. Qu, W. Ji, Y. Zheng, and J. Y. Ying, *Appl. Phys. Lett.* **90**, 133112 (2007).

⁸L. Pan, N. Tamai, K. Kamada, and S. Deki, *Appl. Phys. Lett.* **91**, 051902 (2007).

⁹L. A. Padilha, J. Fu, D. J. Hagan, E. W. Van Stryland, C. L. Cesar, L. C. Barbosa, C. H. B. Cruz, D. Buso, and A. Martucci, *Phys. Rev. B* **75**, 075325 (2007).

¹⁰C. Gan, M. Xiao, D. Battaglia, N. Pradhan, and X. Peng, *Appl. Phys. Lett.* **91**, 201103 (2007).

¹¹M. A. Haase, J. Qui, J. M. DePuydt, and H. Cheng, *Appl. Phys. Lett.* **59**, 1272 (1991).

¹²A. D. Lad, P. P. Kiran, G. R. Kumar, and S. Mahamuni, *Appl. Phys. Lett.* **90**, 133113 (2007).

¹³M. A. Hines and P. Guyot-Sionnest, *J. Phys. Chem. B* **102**, 3655 (1998).

¹⁴B. O. Dabbousi, J. Rodriguez-Viejo, F. V. Mikulec, J. R. Heine, H. Mattoussi, R. Ober, K. F. Jensen, and M. G. Bawendi, *J. Phys. Chem. B* **101**, 9463 (1997).

¹⁵S. Sapra and D. D. Sarma, *Phys. Rev. B* **69**, 125304 (2004).

¹⁶V. V. Nikesh, A. D. Lad, S. Kimura, S. Nozaki, and S. Mahamuni, *J. Appl. Phys.* **100**, 113520 (2006).

¹⁷V. V. Nikesh and S. Mahamuni, *Semicond. Sci. Technol.* **16**, 687 (2001).

¹⁸J. He, Y. Qu, H. Li, J. Mi, and W. Ji, *Opt. Express* **13**, 9235 (2005).

¹⁹A. P. Alivisatos, *Science* **271**, 933 (1996).

²⁰H. S. Brandi and C. B. de Araujo, *J. Phys. C* **16**, 5929 (1983).